

Prospects for searching the $\eta \rightarrow e^+e^-$ rare decay at the CSR^{*}

JI Chang-Sheng(姬长胜) SHAO Ming(邵明)¹⁾ ZHANG Hui(张辉)
CHEN Hong-Fang(陈宏芳) ZHANG Yi-Fei(张一飞)

University of Science and Technology of China, Jinzhai Road 96, Hefei 230026, China

Abstract: We study the possibility of searching the $\eta \rightarrow e^+e^-$ rare decay on the Cooling Storage Ring (CSR) at Lanzhou. The main features of the proposed Internal Target Experiment (ITE) and External Target Facility (ETF) are included in the Monte Carlo simulation. Both the beam condition at the CSR and the major physics backgrounds are carefully taken into account. We conclude that the ITE is more suitable for such a study due to better detector acceptance and higher beam density. At the maximum designed luminosity ($10^{34} \text{ cm}^{-2}\text{s}^{-1}$), $\eta \rightarrow e^+e^-$ events can be collected every ~ 400 seconds at the CSR. With a mass resolution of 1 MeV, the expected signal-to-background (S/B) ratio is around 1.

Key words: η meson, rare decay, CSR, Lanzhou

PACS: 14.40.-n, 29.30.-h, 29.40.-n **DOI:** 10.1088/1674-1137/37/4/046201

1 Introduction

Despite being the most successful theory in particle physics to date, the Standard Model is now being challenged regarding its deficiencies in explaining many aspects, such as the origin of mass, the strong CP problem, neutrino oscillations, matter-antimatter asymmetry, and the origins of dark matter and dark energy [1, 2]. Many theories that lie beyond the Standard Model are proposed, either through extension to super-symmetry, or based on entirely new explanations, such as string theory and extra dimensions. However, which theory is the right one, or at least the “best step” in the right direction, can only be settled experimentally and is one of the most active areas of research in both theoretical and experimental physics.

Rare decay, such as $\eta \rightarrow e^+e^-$, has long been proposed to be a sensitive probe of new physics due to its extremely small branching fraction. As a transition between a pseudoscalar meson and a pair of charged leptons, this process is dominated by the two-photon intermediate state within the framework of the minimal Standard Model [3]. A branching fraction $\eta \rightarrow e^+e^-$ of around 5×10^{-9} is predicted, with a large theoretical uncertainty of one magnitude order (since it is hard to calculate the decay matrix element non-perturbatively) [4]. The hypothetical interactions that arise from physics beyond the Standard Model may significantly change the branching fraction.

An experimental determination of this fraction will on the one hand clarify if there are contributions from exotic decay mechanisms, and on the other hand enable us to gain an understanding of quantum chromodynamics (QCD) in the non-perturbative region.

The $\eta \rightarrow e^+e^-$ rare decay has been searched by several experiments [5, 6], and the latest upper limit on the branching fraction obtained by CLEO-II, $B(\eta \rightarrow e^+e^-) < 7.7 \times 10^{-5}$ [6], is still far from the theoretical expectation. For more than a decade the only experimental proposal to search this rare decay mode has been the WASA at COSY [7], along with its major focus on chiral symmetry and symmetry breaking research. The experiment aims at reaching a sensitivity that allows a test of whether the η decay to the e^+e^- mode occurs at a rate compatible with the Standard Model prediction of 5×10^{-9} . The problem is that only one such rare decay event per week can be found with the current beam luminosity and detector capability.

The Cooling Storage Ring (CSR) [8] in Lanzhou, China, is a heavy-ion facility that can accelerate nuclei up to ^{238}U with a kinetic projectile energy of several hundred MeV to GeV. The CSR can also provide a high-quality proton beam, so both nuclear and hadron physics research can be performed. With a high luminosity beam and properly designed detector system, the search for the $\eta \rightarrow e^+e^-$ rare decay is possible at the CSR. In this work, we study the prospect of such research based on Monte

Received 13 September 2012

* Supported by National Natural Science Foundation of China (10675111, 10835005)

1) E-mail: swing@ustc.edu.cn

©2013 Chinese Physical Society and the Institute of High Energy Physics of the Chinese Academy of Sciences and the Institute of Modern Physics of the Chinese Academy of Sciences and IOP Publishing Ltd

Carlo (MC) simulation. The CSR design parameters and relevant experimental setups are taken into consideration.

2 Experiments at the CSR

Two experimental systems were proposed for hadronic and nuclear physics research at the CSR, namely the Internal Target Experiment (ITE) and the External Target Facility (ETF). The ITE is mainly devoted to hadron physics, while the ETF for nuclear physics at GeV energy.

2.1 The ETF

At present, a phase-I experimental system already exists at the external target area. A schematic setup is depicted in Fig. 1. Along the beam line, after a fixed target a dipole magnetic field is invoked to bend the charged particle tracks. The effective volume of this field is about 1 m long, 1 m wide and 0.3 m high. The strength of the magnetic field can be varied up to about 1.5 Tesla according to the electric current provided. A tracking system with six sets of multi-wire drift chambers (MWDCs) is placed outside the magnetic field to provide hit position measurement for the trajectory of the charged particle. Behind the tracking system is a time-of-flight (TOF) system consisting of three TOF walls. Each TOF wall is a plastic strip array coupled to fast PMTs. The wall size is about 1.4 m². At the far end sits a neutron wall (not shown in the figure) that provides the neutron number trigger and hadron energy measurement.

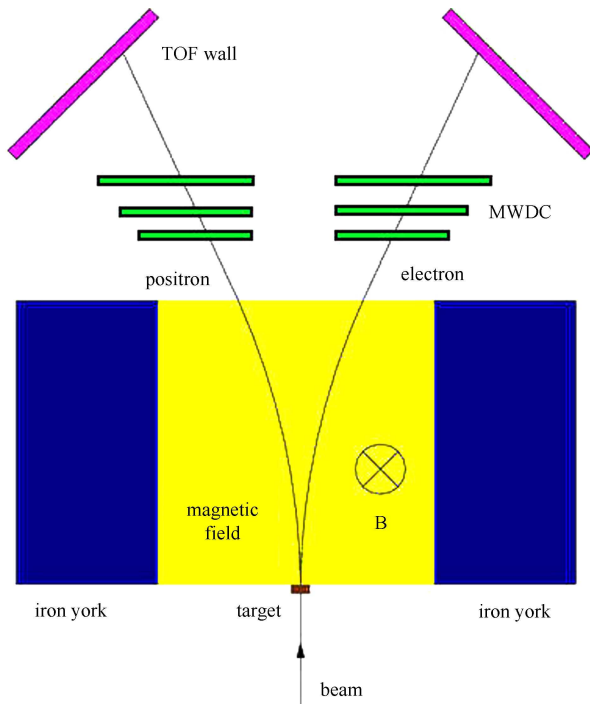


Fig. 1. Schematic of the experimental setup at CSR-ETF.

The ETF system has a planned upgrade to further enhance the research capability, especially in the nuclear physics region. The magnetic dipole field will be enlarged to 1 m×1 m×1 m and more sub-detectors will be added. Since there is no electromagnetic calorimeter or similar detectors in the ETF, the electrons are identified by combining dE/dx measured from the tracking detector and the flight time measured from the TOF detector [9]. To estimate the maximum possibility of searching $\eta \rightarrow e^+e^-$ decay, an ideal case is assumed in the simulation where the tracking system and TOF acceptance are large enough so that any electrons escaping the magnetic field can be measured.

2.2 The ITE

To fully utilize the hadronic research power at the CSR, the ITE has also been proposed. By using the internal pellet target technique, proton-proton or proton-nuclei collisions of very high luminosity can be achieved. As shown in Fig. 2, the proposed experimental system is mainly located in a solenoidal magnetic field, 3 m in length and 1 m in radius. Near the interaction point is the tracking detector that provides both track hits and dE/dx measurement. Surrounding the tracking detector are the TOF and electromagnetic calorimeter, with the same geometric acceptance as the tracking system. There is basically no detector in the backward direction ($>90^\circ$ from the beam direction). In the forward region (not shown in the figure) a hadron calorimeter is foreseen for hadron tagging.

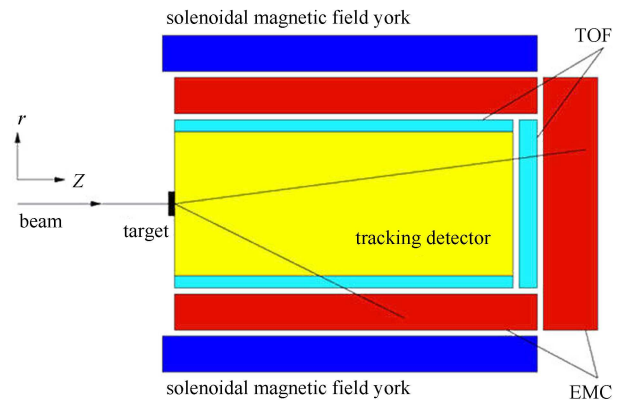


Fig. 2. Schematic of the experimental setup at CSR-ITE.

3 Simulation and formulae

Our study is performed with a fast MC simulation technique. The η mesons from collisions are simulated by an event generator and fed to the detector system. The particle decay and experimental response, such as the trajectory in the magnetic field, multiple scattering, hit generation and digitalization on the detector, are

dealt with by the pseudo-statistical MC method. Major background channels, $\eta \rightarrow \gamma e^+ e^-$, $\eta \rightarrow \gamma \gamma \rightarrow e^+ e^- e^+ e^-$, Δ Dalitz decay and NN bremsstrahlung, are studied. Their yields are calculated as a function of $e^+ e^-$ invariant mass and compared to the expected physics signal ($\eta \rightarrow e^+ e^-$). The prospect of such a study at the CSR is discussed in the next section based on the obtained S/B ratio.

3.1 The event generator

The event generator used in this work is a relativistic transport model (ART1.0) [10], which is dedicated to hadronic reaction simulation in the energy range around several to tens of GeV. This generator can be used in the proton-proton, proton-nuclei and nuclei-nuclei systems, which is suitable for the conditions at the CSR [11].

One of the major background channels, proton-proton bremsstrahlung, cannot be simulated by ART1.0. We use analytic formulae (more details in the background channel subsection) to estimate its contribution.

To search the rare decay $\eta \rightarrow e^+ e^-$ with such a low branching fraction, we need a high production rate, clean signal and low background. For this purpose, a proton beam is favored due to its higher beam density at the CSR and lower combinatorial background compared to heavy-ion collisions with high final state particle multiplicity. The background problem also prevents us from using a target of heavy nuclei, although the cross section is higher.

In this work, when comparing the physics signal and background yields, the collision energy is set to 2.524 GeV, corresponding to a projectile kinetic energy of 1.52 GeV, which is 100 MeV above the $pp \rightarrow pp\eta$ production threshold. At this energy, the $pp \rightarrow pp\eta$ production cross section is near its maximum, while the other η production ($pp \rightarrow \eta X$, X is not pp) probability is relatively small (see Fig. 3). Other center-of-mass (c.m.s.) energies may also be used in specific cases, e.g., a projectile kinetic energy of 2.8 GeV (the maximum energy designed for the CSR) is chosen for detector system simulation in order to test the acceptance for both the ETF and ITE.

3.2 The detector system

The detector system in the MC study is rather simplified - all sub-detectors not directly involved in our study are omitted from the detector system simulation. The detection efficiencies of the detectors used in the MC are assumed to be 100%. For study purposes, the strength of the magnetic field is varied from 0.5 to 2 Tesla, which is beyond the capability of the current (and proposed) magnet system.

A uniform magnetic field is used in the simulation. The charged particles in this field are driven by the Lorentz force, and thus move as helix curves. The multiple-scattering effect during the flight of the particles

is not included in the simulation. When passing the sensitive detectors, the hit information, such as the three-dimensional (3D) hit position and hit time, is recorded for further analysis. Particle decays are only considered at the beginning of the event, so no secondary particles will be produced in flight. We also assume 100% particle identification power for the detector systems.

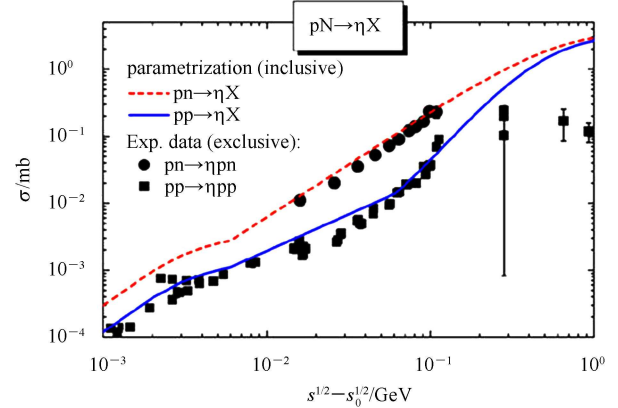


Fig. 3. η production cross section in p+N collisions as a function of c.m.s. energy (\sqrt{s}). s_0 means the η production threshold energy, taken from Ref. [20].

3.3 Background channels

In the energy range 1–2 GeV, the main dilepton sources are the following: $\pi^+ \pi^-$ pair annihilation, π^0 , Δ , η , ω Dalitz decays, NN bremsstrahlung, and direct vector meson decays. For p+p collisions, when focusing on dileptons with invariant mass in the range 0.15–0.9 GeV, only Δ , η , ω Dalitz decays and NN bremsstrahlung are important.

The $pp \rightarrow ppe^+ e^-$ final states are of interest for the search for η rare decay in p+p collisions. Four major background channels are considered in this work, including η Dalitz decay, $\eta \rightarrow \gamma \gamma$, Δ Dalitz decay and NN bremsstrahlung. Their cross sections are estimated as a function of the $e^+ e^-$ invariant mass, either by analytic formulae or fast simulation.

3.3.1 η Dalitz decay

The η Dalitz decay $\eta \rightarrow \gamma e^+ e^-$ is an inevitable background channel for the $\eta \rightarrow e^+ e^-$ rare decay search. The γ in the η Dalitz decay may escape the experiment's detection, either by being outside the detector acceptance or being too inefficient to be detected, so we observe the same final states as the signal channel. The γ can also be converted to an $e^+ e^-$ pair, forming a final state of $ppe^+ e^- e^+ e^-$. This contribution is similar to the $\eta \rightarrow \gamma \gamma$ background channel discussed later in this paper (although their phase spaces are a little different), and is not included in this work.

The contribution from the η Dalitz decay takes the form [12]

$$\begin{aligned} \frac{d\sigma}{dM^2} \Big|_{\eta \rightarrow \gamma e^+ e^-} &= \sigma_\eta(s) \frac{2\alpha}{3\pi M^2} \sqrt{1 - \frac{4m_e^2}{M^2}} \left(1 + \frac{2m_e^2}{M^2}\right) \\ &\times B^{\eta \rightarrow \gamma\gamma} F_\eta^2(M^2) \left(\frac{\lambda(m_\eta^2, M^2, 0)}{\lambda(m_\eta^2, 0, 0)}\right)^{3/2}, \end{aligned} \quad (1)$$

where \sqrt{s} is the c.m.s. energy of the proton-proton collision, M is the invariant mass of the e^+e^- pair, and m_e is the remaining mass of the electron. $\sigma_\eta(s)$ is the total η -production cross section, which is not parameterized but obtained directly from the ART1.0 event generator. For p+p collisions at a c.m.s. energy of 2.524 GeV, this is around 0.1 mb. $B^{\eta \rightarrow \gamma\gamma}$ denotes the branching fraction of $\eta \rightarrow \gamma\gamma$, which is 0.39 (from the Particle Data Group [14]). The form factor $F_\eta^2(M^2)$ is taken from the vector meson dominance model (VMD) parameterizations, $F_\eta^2(M^2) = \left(1 - \frac{M^2}{A_\eta^2}\right)^{-1}$, with $A_\eta = 0.72$ GeV [12, 13]. The kinematic function λ reads

$$\lambda(x, y, z) = x^2 + y^2 + z^2 - 2(xy + yz + zx). \quad (2)$$

3.3.2 $\eta \rightarrow \gamma\gamma$

η produced in p+p collisions has a significant branching fraction (39%) to decay into an $\gamma\gamma$ pair. These γ s may both be converted to a e^+e^- pair when interacting with the materials in the experimental system, forming a final state of $ppe^+e^-e^+e^-$. The detector system possibly misses one electron and one positron in the final states (so we “see” ppe^+e^-), and thus also contributes to the background. Such a background type relies on a practical experimental setup, since the occurrence of γ conversion depends sensitively on detailed detector material placement. For this background channel, only the ITE detector system is considered. Since the tracking system in ITE is able to effectively remove γ conversions far from the interaction point (IP) by reconstructing the displaced secondary vertex (or the distance of the closest approach to the event vertex), we focus on the events with both γ converted very near to the IP, i.e. the γ conversions take place at the beam pipe.

In most high-energy experiments, a beryllium (Be) beam pipe is used at the IP region. For γ s with energy well above the pair production threshold ($2m_e$), the conversion cross section for Be is 0.178b. If we take the thickness of the Be pipe to be 2 mm, the probability for one γ conversion is 0.44%, and $\sim 2 \times 10^{-5}$ for two γ conversions in an $\eta \rightarrow \gamma\gamma$ event.

$pp \rightarrow pp\eta \rightarrow ppe^+e^-e^+e^-$ events are simulated using the same procedure we use to process $\eta \rightarrow e^+e^-$ decays. We assume that the γ conversion vertex is the same as the event vertex, and the decays of $\eta \rightarrow \gamma\gamma$ and $\gamma \rightarrow e^+e^-$

simply follow isotropic phase space distribution (in the remaining frame of the decay particles). The responses of the experimental system to the final state particles are simulated, and only the events with the four required particles (ppe^+e^-) detected are selected and further analyzed.

3.3.3 Δ Dalitz decay

The Δ Dalitz decay contributes to the background by the reaction of $pp \rightarrow p\Delta^+$ and $\Delta^+ \rightarrow pe^+e^-$, with the same final states as $pp \rightarrow pp\eta \rightarrow ppe^+e^-$.

The cross section of the Δ Dalitz decay can be written as follows: [15, 16]

$$\begin{aligned} \frac{d\sigma}{dM^2} \Big|_{\Delta \rightarrow Ne^+e^-} &= \int_{(m_N+m_\pi)^2}^{(\sqrt{s}-m_N)^2} dM_\Delta^2 \sigma_\Delta(s, M_\Delta) D(M_\Delta) \\ &\times \frac{1}{\Gamma_\Delta} \left(\frac{d\Gamma}{dM^2}\right)^{\Delta \rightarrow Ne^+e^-}. \end{aligned} \quad (3)$$

M is the invariant mass of the e^+e^- pair, M_Δ and Γ_Δ are the mass and full width of the intermediate Δ , $\sigma_\Delta(s, M_\Delta)$ is the production cross section of Δ at given mass M_Δ , and $D(M_\Delta)$ is the weight function. The total Δ -production cross section is given by

$$\sigma_\Delta(s) = \int_{(m_N+m_\pi)^2}^{(\sqrt{s}-m_N)^2} dM_\Delta^2 \sigma_\Delta(s, M_\Delta) D(M_\Delta).$$

The last term in the equation

$$\frac{1}{\Gamma_\Delta} \left(\frac{d\Gamma}{dM^2}\right)^{\Delta \rightarrow Ne^+e^-}$$

describes the differential width of the Δ decays into a e^+e^- pair.

The equation above contains two parts, one for Δ production and the other for Δ Dalitz decay. Though the production of Δ s in p+p collisions can be analytically parameterized, in this work the simulated Δ s are directly produced from the event generator. The mass spectra of Δ from ART1.0 is illustrated in Fig. 4. The total Δ -production cross section in p+p collisions at 2.524 GeV is taken as 16 mb [17]. (This may be overestimated, but can serve as the worst-case background.) For the other part, the differential width of the Δ Dalitz decay is given by

$$\frac{1}{\Gamma_\Delta} \left(\frac{d\Gamma}{dM^2}\right)^{\Delta \rightarrow Ne^+e^-} = \frac{\alpha}{3\pi M^2} B^{\Delta \rightarrow N\gamma}(M_\Delta) R_F^\Delta(M_\Delta, M), \quad (4)$$

where $B^{\Delta \rightarrow N\gamma}(M_\Delta)$ stands for the branching ratio of the electromagnetic width to the total Δ decay width, $R_F^\Delta(M_\Delta, M)$ is the ratio of the electromagnetic Δ decay widths for virtual to real photons. $B^{\Delta \rightarrow N\gamma}(M_\Delta)$ is taken

as 0.6% [14] independent of M_Δ , and

$$\begin{aligned}
 & R_T^\Delta(M_\Delta, M) \\
 &= \frac{\Gamma_Y^{\Delta \rightarrow \gamma^* N}(M_\Delta, M)}{\Gamma_Y^{\Delta \rightarrow \gamma^* N}(M_\Delta, 0)} \\
 &= \frac{M_\Delta M^2 + 5M_\Delta q_0^2 - 3M^2 m_N - 3M^2 q_0 - 3m_N q_0^2 - 3q_0^3}{q_0^2(5M_\Delta - 3m_N - 3q_0)} \\
 &\quad \times (\lambda(M_\Delta^2, m_N^2, M^2) / \lambda(M_\Delta^2, m_N^2, 0))^{1/2}, \quad (5)
 \end{aligned}$$

with $q_0 = (M_\Delta^2 + M^2 - m_N^2) / (2M_\Delta)$ and $\lambda(x, y, z)$ from Eq. (2).

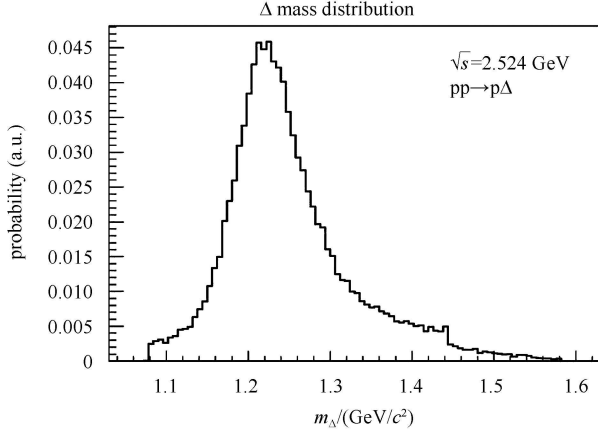


Fig. 4. The Δ mass spectral distribution obtained in p+p collisions at c.m.s. energy $\sqrt{s}=2.524$ GeV, simulated by ART1.0.

3.3.4 NN bremsstrahlung

NN bremsstrahlung is also a major background channel. The bremsstrahlung cross section in NN collisions is significant and the radiation of virtual photons may occur, producing the $pp \rightarrow pp\gamma^* \rightarrow ppe^+e^-$ final state. Predictions of this process from different theoretical models may vary by an order of magnitude.

In this work, we choose the formulae based on the soft-photon approximation (SPA) method as described in reference [18–20]. The SPA is based on the assumption that the radiation from internal lines is negligible and the strong interaction vertex is on-shell. In this case the strong interaction part and the electromagnetic part can be separated. For proton-neutron reaction, the differential cross section for $pn \rightarrow pne^+e^-$ can be written as

$$\frac{d\sigma}{dydq^2q_T dM} = \frac{\alpha^2}{6\pi^2} \frac{\sigma_1(s)}{Mq_0^2} \frac{R_2(s_2)}{R_2(s)}, \quad (6)$$

$$R_2(s) = \sqrt{1 - (m_n + m_p)^2 / s}, \quad (7)$$

$$s_2 = s + M^2 - 2q_0\sqrt{s}, \quad (8)$$

$$\sigma_1(s) = \frac{s - (m_p + m_n)^2}{2m_p^2} \sigma(s), \quad (9)$$

where m_p and m_n are the mass of the (projectile) proton and neutron; M , q_0 , q_T and y are the invariant mass, energy, transverse momentum and rapidity of the dilepton pair, respectively; and $\sigma(s)$ is the on-shell elastic cross section for the proton-neutron reaction. At a c.m.s. energy of 2.524 GeV, the elastic p+n cross section is taken as 20 mb. For the proton-proton reaction, the bremsstrahlung cross section is much lower [21], and taken as one-tenth of that in the proton-neutron reaction.

By integration over y and q_T in Eq. 6, the cross section $d\sigma/dM^{pn \rightarrow pne^+e^-}$ can be obtained. At the given energy (2.524 GeV), this integration is done numerically since the allowed phase space of the dilepton pair depends on the collision energy and y , q_T are correlated.

4 Simulation results and discussions

4.1 Detector systems

To search a rare decay with such a low branching fraction, the detector system should have large acceptance, high efficiency, good track-reconstruction quality and clean particle identification (PID). Large acceptance and high efficiency are helpful in increasing the sample statistics, or decreasing the run time needed, while a good track-reconstruction quality and clean PID are crucial for background suppression. To estimate the acceptance of the ETF or ITE system, an η meson is emitted from the target position. The η momentum is randomly distributed in the 0–2 GeV/c range at a fixed direction along the beam line. The η s are assumed to decay 100% to e^+e^- pairs. As shown in Fig. 5, the η reconstruction efficiency at ETF is plotted as a function of η momentum, for four sets of magnetic field strength, namely 0.5, 1, 1.5 and 2 Tesla. The reconstruction efficiency is defined as the ratio of the number of η s (as a function of momentum) with both daughters detected by TOF over the total number of η s produced in the event. One can find that at a high momentum region (around 2 GeV/c), the efficiency decreases with the increase in magnetic field strength. This is intuitive since a stronger field bends charged particles more, so the decay electrons or positrons (they move almost along the η momentum direction due to high Lorentz boost) have less chance to escape the magnetic field volume and hit the TOF. However, at a low momentum region, the η reconstruction efficiency increases at first, and then decreases with increasing magnetic field strength. This is also understandable since at low η momentum, the decay electron and positron move in nearly opposite directions. At a low magnetic field strength ($B \rightarrow 0$) they are hard to be detected simultaneously by the TOF (e.g. at $B=0$ and $p=0$ the efficiency must be 0). If the magnetic field

is too strong, the efficiency is also low since the decay electron or positron does not have enough momentum to escape the field. Considering the η phase space from the ART1.0 generator, with an average momentum at ~ 0.5 GeV/c, the η reconstruction efficiency is no more than a few per cent, even at the optimized magnetic field strength $B=1.5$ T.

ART1.0 simulated events of the proton-proton reaction at a projectile kinetic energy of 2.8 GeV are then fed into the ETF simulation framework. It is found that the η reconstruction efficiency is less than 1%. (Note: the efficiency from Fig. 5 is obtained with η s emitted in the beam direction, while here the η phase space is determined by an event generator.) Furthermore, the beam density at ETF is much lower than that at ITE by about 3–4 magnitudes. So we conclude that it is not promising to search the $\eta \rightarrow e^+e^-$ rare decay at the CSR-ETF due to limited detector acceptance and low beam density.

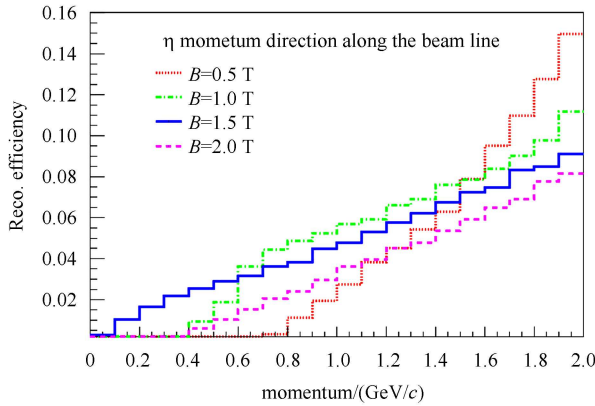


Fig. 5. η reconstruction efficiency as a function of momentum (p) at the ETF. The η is emitted along the beam direction with momentum ranging from 0–2 GeV/c. The magnetic field strength varies from 0.5–2 T.

Similar simulation processes are applied for the ITE system. In Fig. 6 we show the η reconstruction efficiency at ITE as a function of η momentum, and at four different magnetic field strengths. A slight difference from Fig. 5 is that the η s are emitted from proton-proton collisions at a projectile kinetic energy of 2.8 GeV. One can find that the efficiency increases with η momentum and is saturated for those with a momentum larger than 1 GeV/c. The saturation efficiency is about 90% at $B=0.5, 1.0, 1.5$ Tesla, but drops slightly to less than 80% at $B=2.0$ Tesla. In any case, the reconstruction efficiency is much higher than that at ETF. Considering the much higher beam density at ITE, it may be a more suitable place to search the η rare decay than ETF.

We can further quantitatively estimate the event rate of the $\eta \rightarrow e^+e^-$ decay at ITE. The pellet target proposed at ITE has an effective thickness of 10^{15} – 10^{16} atoms/cm²,

and the designed proton beam intensity is 10^{10} – 10^{12} pps. Thus the luminosity is about 10^{31} – 10^{32} cm⁻²s⁻¹. The maximum designed luminosity is 10^{34} cm⁻²s⁻¹. If we take the η production cross section $\sigma_{pp \rightarrow p\eta} = 0.1$ mb, the $\eta \rightarrow e^+e^-$ branching fraction to be 5×10^{-9} , and the total η reconstruction efficiency of the detector system to be 50%, then the mean time to get each $\eta \rightarrow e^+e^-$ rare decay event at the ITE is about 40000 seconds (for 10^{32} cm⁻²s⁻¹ luminosity). This time will decrease to only 400 seconds at maximum CSR luminosity. In such a case, thousands of η rare decays can be collected in only several weeks of a CSR proton-proton run.

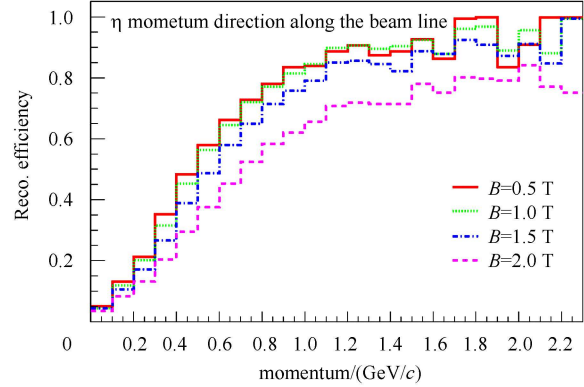


Fig. 6. η reconstruction efficiency as a function of momentum (p) at ITE. η s are produced in p+p collisions with a projectile kinetic energy of 2.8 GeV. The magnetic field varies from 0.5–2 Tesla.

4.2 Backgrounds

The cross sections of four main background channels are illustrated in Figs. 7, 8, 9 and 10, as a function of the invariant mass of e^+e^- pairs. The reaction system is fixed to be proton-proton at a c.m.s. energy of 2.524 GeV. One can find that the differential cross section for all these background channels near η mass is on the order of the 10^{-7} mb level. Since the η production rate used is 0.1 mb and the $\eta \rightarrow e^+e^-$ decay branching fraction is on the order of 10^{-9} , the mass resolution at ITE should reach about 1 MeV so that this rare decay can be observed. This is shown in detail in Fig. 11, where the cross section of the $\eta \rightarrow e^+e^-$ signal is plotted along with the background channels. Four different mass reconstruction resolutions are studied by smearing the $\eta \rightarrow e^+e^-$ signal with a Gaussian distribution. It is obvious that the S/B ratio increases with better mass resolution. With a mass resolution of 1 MeV

$$\left(\frac{\delta M}{M} \sim 0.2\% \right),$$

the S/B ratio can be as high as around 1.

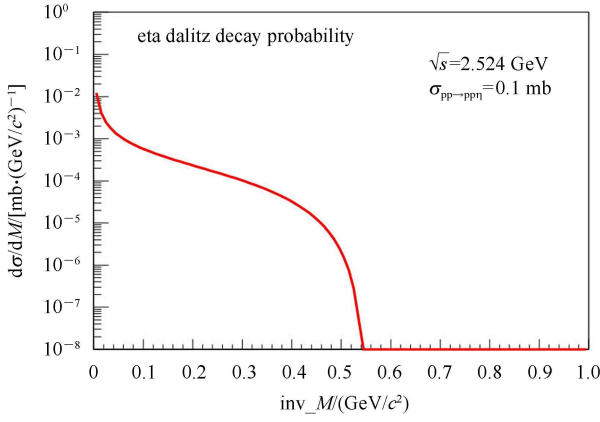


Fig. 7. η production and Dalitz decay cross section in p+p collisions at $\sqrt{s}=2.524$ GeV, as a function of the invariant mass of final-state e^+e^- pairs.

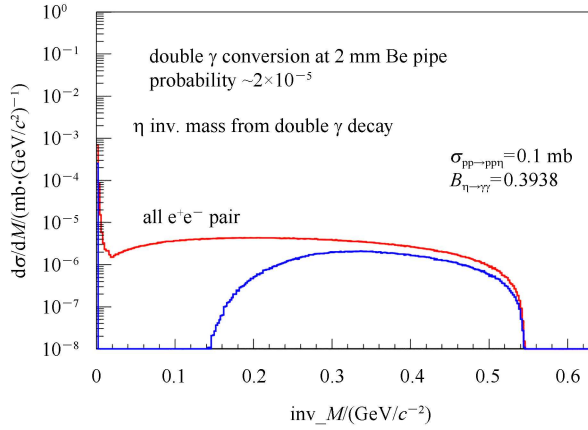


Fig. 8. η double- γ conversion cross sections in p+p collisions at $\sqrt{s} = 2.524$ GeV, as a function of the invariant mass of final-state e^+e^- pairs. The probability of both γ s being converted into e^+e^- pairs at a 2 mm thick Be beam pipe is assumed to be 2×10^{-5} . The red line represents all e^+e^- pairs, while the blue line indicates pairs from different converted γ s.

All four of these background channels can be carefully studied with the same setup at ITE, which is also important before we can really start to search the $\eta \rightarrow e^+e^-$ decay. The study of these background channels serves as a necessary baseline for further research.

The most profound background channel is the proton-proton bremsstrahlung. However, this background can be suppressed by choosing a proper phase space of the reconstructed e^+e^- pair, since in proton-proton bremsstrahlung the virtual γ is dominantly emitted along the beam direction, while for $pp \rightarrow pp\eta$ the η phase space distribution is very different. For the Δ Dalitz decay, the difference in the phase space of the final state particle is less distinguishable from the real signal, demanding a careful study of this decay mode beforehand.

The other two background channels are inevitable, although for double γ conversion the contribution can be

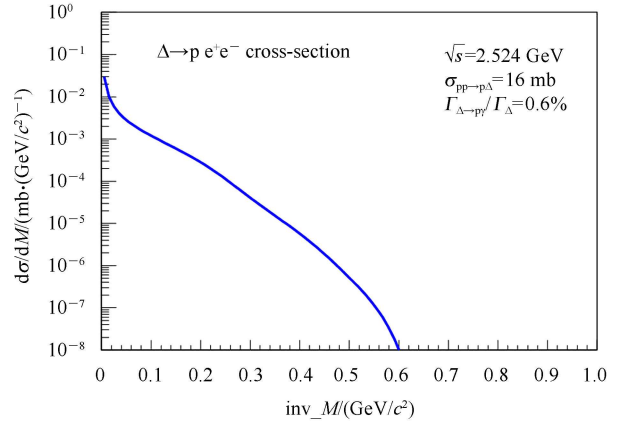


Fig. 9. Δ Dalitz decay cross section in p+p collisions at $\sqrt{s} = 2.524$ GeV, as a function of the invariant mass of final-state e^+e^- pairs.

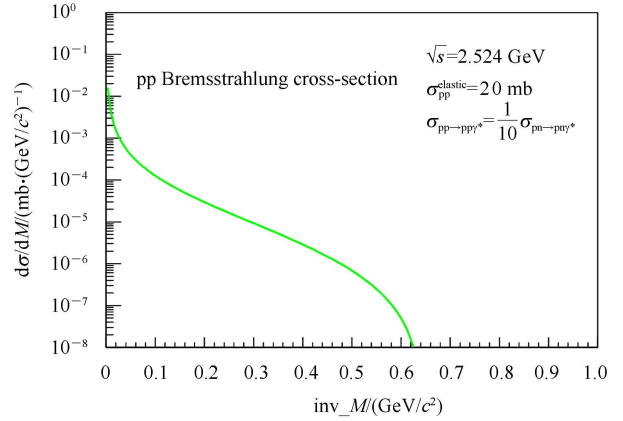


Fig. 10. Bremsstrahlung cross section in p+p collisions at $\sqrt{s} = 2.524$ GeV, as a function of the invariant mass of the final-state e^+e^- pairs.

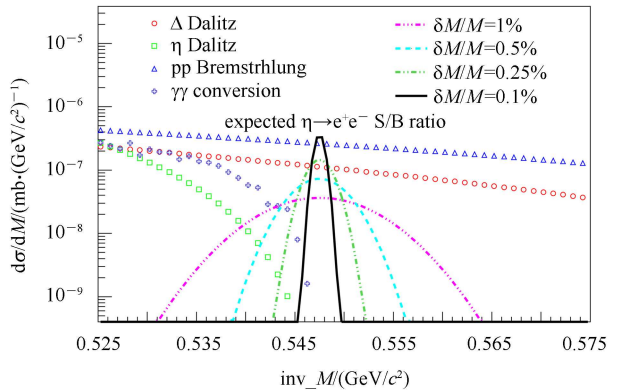


Fig. 11. Expected signal and major background cross section in p+p collisions at $\sqrt{s}=2.524$ GeV, as a function of the invariant mass of the final-state e^+e^- pairs.

somewhat suppressed by precisely constructing the conversion vertex. To better distinguish the signal, it is important to improve the mass resolution. Since the EMC used in ITE is limited in its resolution, even using the most advanced techniques (e.g. a full homogenous crystal calorimeter), the requirements for track momentum reconstruction (especially for electrons and positrons), as well as beam quality, must be very stringent. New cutting-edge tracking detector technology may be necessary.

5 Summary

An MC simulation was performed to search the $\eta \rightarrow e^+e^-$ rare decay mode on the ITE and ETF experimental systems by using p+p collisions slightly above the η production threshold at the CSR. The main fea-

tures of the experiments and beam condition at the CSR are taken into account. Four major physics backgrounds, namely η Dalitz decay, $\eta \rightarrow \gamma\gamma$, Δ Dalitz decay and NN bremsstrahlung, are carefully estimated. We conclude that the ITE is more suitable for such a study due to larger detector acceptance and higher beam density. Proper detector system design and excellent performance are needed to better distinguish the $\eta \rightarrow e^+e^-$ signal from the backgrounds. At the maximum designed luminosity ($10^{34} \text{ cm}^{-2}\text{s}^{-1}$), $\eta \rightarrow e^+e^-$ events can be collected every ~ 400 seconds at the CSR. With a mass resolution of 1 MeV, the expected S/B ratio is around 1.

We wish to thank Prof. H.S. Xu, Z.G. Xiao and Z.Y. Sun for valuable discussions on the experiments at the CSR.

References

- 1 John Ellis. Nature, 2007, **448**: 297
- 2 Paul Langacker. The Standard Model and Beyond (Series in High Energy Physics, Cosmology and Gravitation). Taylor & Francis. 2009
- 3 Bergström L. Z. Phys. C, 1982, **14**: 129
- 4 Landsberg L G. Phys. Rep., 1985, **128**: 301
- 5 White D B, Tippens W B, Abegg R et al. Phys. Rev. D, 1996, **53**: 6658
- 6 CLEO collaboration. Phys. Rev. D, 1997, **56**: 5359
- 7 WASA-at-COSY collaboration. Proposal for the Wide Angle Shower Apparatus (WASA) at COSY-Jülich, arXiv:nucl-ex/0411038v1
- 8 ZHAN W L et al. Nucl. Phys. A, 2008, **805**: 533c
- 9 SHAO M, Barannikova O, DONG X et al. Nucl. Instrum. Methods. A, 2006, **558**: 419
- 10 LI B A, KO C M. Phys. Rev. C, 1995, **52**: 2037
- 11 LUO X F, DONG X, SHAO M et al. Phys. Rev. C, 2007, **76**: 044902
- 12 Ernst C, Bass S A, Belkacem M et al. Phys. Rev. C, 1998, **58**: 447
- 13 NA60 collaboration. Phys. Lett. B, 2009, **677**: 260
- 14 Review of Particle Physics. J. Phys. G, 2010, **37**: 075021
- 15 Titov A I, Kämpfer B, Bratkovskaya E L. Phys. Rev. C, 1995, **51**: 227
- 16 Ernst C, Bass S A, Belkacem M et al. Phys. Rev. C, 1998, **58**: 447
- 17 VerWest B J, Arndt R A. Phys. Rev. C, 1982, **25**: 1979
- 18 Gale C, Kapusta J. Phys. Rev. C, 1987, **35**: 2107
- 19 Ernst C et al. Phys. Rev. C, 1998, **58**: 447
- 20 Bratkovskaya E L, Cassing W. Nuclear Physics A, 2008, **807**: 214
- 21 Schäer M, Biro T S, Cassing W, Mosel U. Phys. Lett. B, 1989, **221**: 1